The Behavior of Jordanian Oil Shale during Combustion Process from the El-Lajjun Deposit

Mousa Gougazeh[1*], Sameh Alsaqoor[2], Gabriel Borowski[3],
Ashraf Alsafasfeh[1], Ismail I. Hdaib[4]

[1] Department of Natural Resources and Chemical Engineering, Tafila Technical University, P.O. Box 179, Tafila 66110, Jordan

[2] Department of Mechanical Engineering, Tafila Technical University, P.O. Box 179, Tafila 66110, Jordan

[3] Environmental Engineering Faculty, Lublin University of Technology, ul. Nadbystrzycka 40B, 20-618 Lublin, Poland

[4] Department of Renewable Energy Engineering, Isra University, Amman 11622, Jordan

* Corresponding author's e-mail: mgougazeh99@gmail.com

ABSTRACT

The results of X-ray diffraction, thermogravimetric and FTIR spectroscopy analyses of mineral composition indicated that the El-Lajjun oil shale is principally composed of calcite, quartz with minor amounts of kaolinite), gypsum, and apatite. The obtained oil shale ash products at 830 °C and 1030 °C are dominated by lime, quartz, anhydrite, portlandite, gehlenite, and amorphous phases. The TGA weight loss curves clearly indicate that it occurred in the temperature range from 310 to 650 °C. The decomposition of oil shale carbonates was detected above 750°C. The functional groups in the organic material of oil shale are dominated by the aliphatic hydrocarbons, the semi-ash of which had diverse structures of polycyclic aromatic hydrocarbons. The most intensive of combustion occurred in the temperature range of 400–750 °C. In this temperature range, about 75 wt.% was accounted for the total mass loss.

Keywords: El-Lajjun oil shale; combustion; X-ray diffraction, thermogravimetric, fourier transform infrared spectroscopy; X-ray fluorescence.

INTRODUCTION

Oil shale is defined as a sedimentary rock that contains a solid combustible organic matter in a mineral matrix, Oil shale contains an organic matter in the form of kerogen. The other part called bitumen is an inorganic soluble inorganic solvents, but its total amount in organic matter is small (Hruljova et al., 2013; Larsen et al., 2000). Jordanian oil shale consists of thick bedded or concretionary limestone; sometimes dolomite and chert are entangled in the oil shale sequence, and phosphate layer occurs usually under the oil shale deposits. It belongs to the upper Cretaceous and lower Tertiary formations (Abed et al., 2009).

Jordan has limited energy resources, such as crude oil or natural gas, compared to its neighboring countries. However, oil shale is an important and unused energy source in the country. Oil shales in Jordan are widespread. Enormous reserves are present in central Jordan east of Karak and Tafila (e.g. Lajjun, Attarat, Jurf Ed Darawiesh, Sultani, etc.), north and northwestern Jordan north and west of Irbid (Magarin, Wadi Shallaleh, Taibeh, and Hammeh), and in the subsurface in the Azraq Basin (Bender, 1974). The deposits in central Jordan have received and still receive most of the attention in the last 4 decades (Hamarneh, 1988). The oil shale covers a wide area (>70 billion tons) in Jordan from north to south (Bseieso, 2003), and it gives a considerable added value to the Jordanian economy by preventing the importation of demand oil, energy, and development of the country.

Several investigations have been conducted into Jordanian shale on the parameters of the operation for the use of oil shale. All of these investigations concentrated on the organic part of the oil shale for use as an alternative to oil (Khraisha et al., 2003; Shaohui, 2000). However, there are few works that deal with the utilization of fly ash produced as waste from the different oil shale industries, which represents more than 50% of the total amount of processed raw oil shale. A large amount of ash represents a great environmental concern and one of the most important hindrances which contribute negatively to the utilization of oil shale. The present work is concentrated on the mineralogical, chemical, physical, and thermal behaviors of the Jordanian oil shale and the composition of their obtained ashes at different temperatures for economic potential.

MATERIALS AND METHODS

Materials

The present study was conducted on the collected representative samples from the El-Lajjun deposit, central part of Jordan (Figure 1). The obtained samples were reduced by a jaw crusher and then sieved into different grain sizes. The sample size of less than 1000 μm was used in the combustion (burning) process. Standard Pt crucibles were used, and the mass of samples was 50 g oil shale
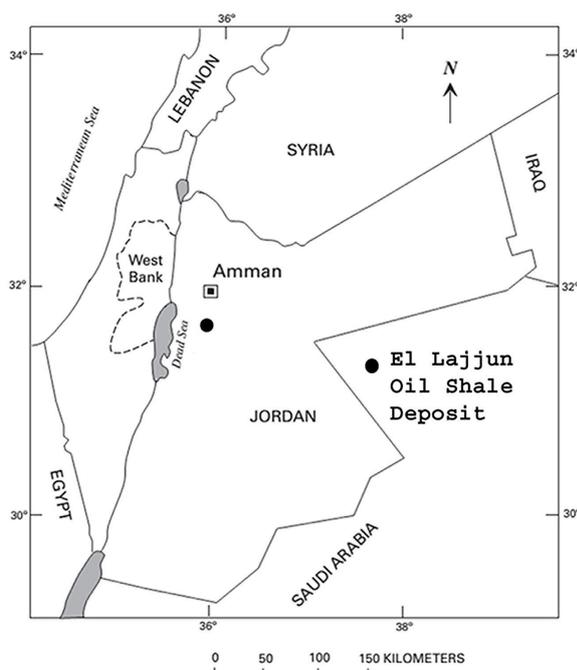

Figure 1. Location map of the study area

with size less than 1000 μm. At different burning temperatures 525, 650, 750, 830, and 1030 °C, the oil shale ash (OSA) was produced in a laboratory muffle furnace under atmospheric conditions. These burning tests were performed in air at 10 °C min⁻¹ heating rate up to 525 °C in 40 minutes, and the samples were heated for 1 h for the temperature intervals (525 to 650 °C, 525 to 750 °C, 525 to 830 °C, and 525 to 1030 °C). When each sample reached 525 °C, 650 °C, 750 °C, 830 °C, and 1030 °C, they were maintained for 3h each and then cooled for 6h to obtain full combustion to remove incorporated hydrocarbons.

Characterization methods

At the Institute of Mineralogy and Institute of building materials, Leibniz University Hannover, Germany, the oil shale and their oil shale ashes (OSA) were investigated in terms of mineralogy, chemistry, grain size and thermal analyses.

The Malvern Master Sizer Model 2605, a laser diffraction particle sizer was used to measure the particle size distributions for the oil shale and oil shale ash. The major oxides of oil shale and oil shale ash (at 830°C) were determined using a Philips PW1400 Wavelength Dispersive Sequential X-ray fluorescence (XRF) Spectrometer at the Natural Resources Authority, Amman, Jordan. A Bruker AXS D4 ENDEAVOR diffractometer with Cu Kα radiation and a Ni filter (operated at 40 kV, 40 mA in 2-72 °2θ region with a scan step of 0.03 °2θ and a count time of 5 s per step) was used to identify the mineralogical phase of the investigated oil shale samples and their oil shale ash. The differential thermal analysis (DTA) and thermogravimetric analysis (TGA) were performed using a Setaram Setsys EV 1750 Thermal Analyzer (Germany) at a heating rate of 4 °C/min from ambient temperatures to 1200 °C with corundum (Al₂O₃) as the inert standard. The measurements under were performed flowing He atmosphere (20 ml/min). A Bruker IFS66v FTIR spectrometer, equipped with the Bruker OPUS software package was used to record the infrared spectra of the oil shale samples and their oil shale ashes (the KBr pellets were prepared from each sample using 1 mg of oil shale or oil shale ash samples, mixed with 200 mg KBr in an agate mortar, and was then pressed into pellets 13 mm in diameter with a pressure of 8.0 MPa, the spectra were recorded over the range of 4000–300 cm⁻¹). A JEOL JSM-6390A system, together with

the EDX analyzer, was used to study the samples of oil shale and oil shale ash by scanning electron microscopy (SEM). The SEM investigations were operated at acceleration voltages of 20 kV (the produced ashes were analyzed both as dispersed powder and prepared with the help of conductive graphite pads on Al sample holders, a thin coating of Au was generated on each specimen by sputtering with an Edwards SCANCOAT SIX sputter coater).

RESULTS AND DISCUSSION

Granulometric analysis

Figure 2 shows the distribution of particle size for both oil shale and oil shale ash at 830 °C. It was clearly noted that the distribution is very similar to the particle size of both curves. These results reflect that the occurrence of very fine fragmentation particles of ash due to the combustion phase of oil shale in the laboratory furnace.

Chemical analysis

The major oxides of both oil shale and oil shale ash that were analyzed using XRF are listed in Table 1. The major oxides found are calcium and silica. Table 1 shows that the main oxides are CaO (31.20 wt.%), SiO_2 (18.50 wt.%), SO_3 (4.30 wt.%), Al_2O_3 (3.60 wt.%), P_2O_5 (3.50 wt.%), Fe_2O_3 (1.70 wt.%), MgO (1.30 wt.%), TiO_2 (0.2 wt.%), Na_2O (0.2 wt.%) and K_2O (0.1 wt.%). The high percentage (37.50 wt.%) of loss on ignition (LOI) of the studied oil shale is associated with CO_2 and H_2O, which appeared by decomposition of the

Table 1. Chemical analysis of oil shale and oil shale ash by XRF

Oxide (wt. %)	Oil shale (OS)	Oil shale ash (OSA)
SiO_2	18.50	26.40
TiO_2	0.20	0.30
Al_2O_3	3.60	6.20
Fe_2O_3	1.70	2.40
CaO	31.20	44.20
MgO	1.30	1.80
Na_2O	0.20	0.30
K_2O	0.10	0.40
SO_3	4.30	7.50
P_2O_5	3.50	5.20
LOI*	37.30	5.80

* LOI – loss on ignition.

carbonate and kaolinite minerals, respectively, in addition to the percentage of organic carbon.

It was noted that the oil shale and the produced oil shale ash vary markedly in their contents of SiO_2, CaO, Al_2O_3, Fe_2O_3, SO_3, and P_2O_5 as well as LOI. The content of SiO_2, CaO, Al_2O_3, Fe_2O_3, SO_3, and P_2O_5 increases sharply in the oil shale ash (26.4 wt.%, 44.2 wt.%, 6.2 wt.%, 2.4 wt.%, 7.5 wt.%, and 5.2 wt.%, respectively), while LOI shows a significant decrease during the ashing phase at high-temperature (830 °C) due to the complete decomposition of carbonate minerals. The presence of SO_3 suggests that CaO may be responsible for retaining sulfur in ash as $CaSO_4$ (Saikia et al., 2015a). The mineral composition of the analyzed oil shale ash at different temperaures were refleted by silica, alumina, and calcium contents, as detected by the XRD (Figure 3).
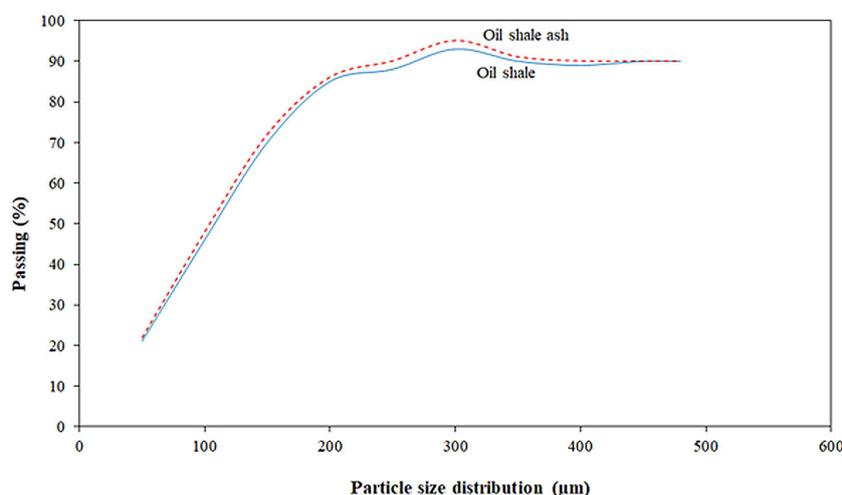

Figure 2. Distribution of particle size for both oil shale and oil shale ash at 830 °C

X-ray diffraction (XRD) analysis

Table 2 and Figure 3 show the effect of different burning temperatures (525, 650, 830, and 1030 °C) on the mineral content of oil shale.

The oil shale samples were mainly composed of calcite, followed by quartz. As it was shown in Figure 3, there were traces of gypsum, kaolinite, apatite (fluorapatite), and iron oxides. It is clear from the XRD spectra that at a temperature of 525 °C, the heated oil shale consisting mainly of calcite, quartz, kaolinite, and apatite. This is due to the crystalline structure of calcite had not been decomposed and the hydroxyl reaction of kaolinite is not characteristic. The results showed that the most distinguishing peaks of calcite mineral are detected at 3.36 Å, 3.035 Å, 2.495 Å, 2.285 Å, 2.095 Å, 1.913 Å, 1.875 Å, and 1.604 Å (Gougazeh, 2022). The peaks of quartz mineral are observed at 4.26 Å and 3.35 Å (Gougazeh and Buhl 2010). The kaolinite peaks are detected at 7.17 Å, 3.58 Å, and 1.49 Å (Gougazeh, 2020), while those at 2.8 Å and 2.702 Å are the distinctive peaks of apatite (Gougazeh, 2022).

Table 2. Effect of different heating temperatures on the mineral content for both oil shale raw material and the obtained oil shale ash

Mineral	OS	OSA, 525 °C	OSA, 650 °C	OSA, 830 °C	OSA, 1030 °C
Calcite	xxxx	xxxx	xxxx	x	-
Quartz	xx	xx	xx	xx	xx
Kaolinite	x	x	-	-	-
Metakaolin	-	-	x	x	x
Apatite	x	x	x	x	x
Gypsum-Anhydrite	x (gypsum)	xx (anhydrite)	xx (anhydrite)	xx (anhydrite)	xx (anhydrite)
Magnetite	x	x	x	x	-
Illite-Muscovite	x	x	x	x	-
Lime	-	-	-	xx	xxx
Portlandite	-	-	-	x	xx
Gehlenite	-	-	-	x	xx
Amorphous phases	-	-	x	xx	xxxx

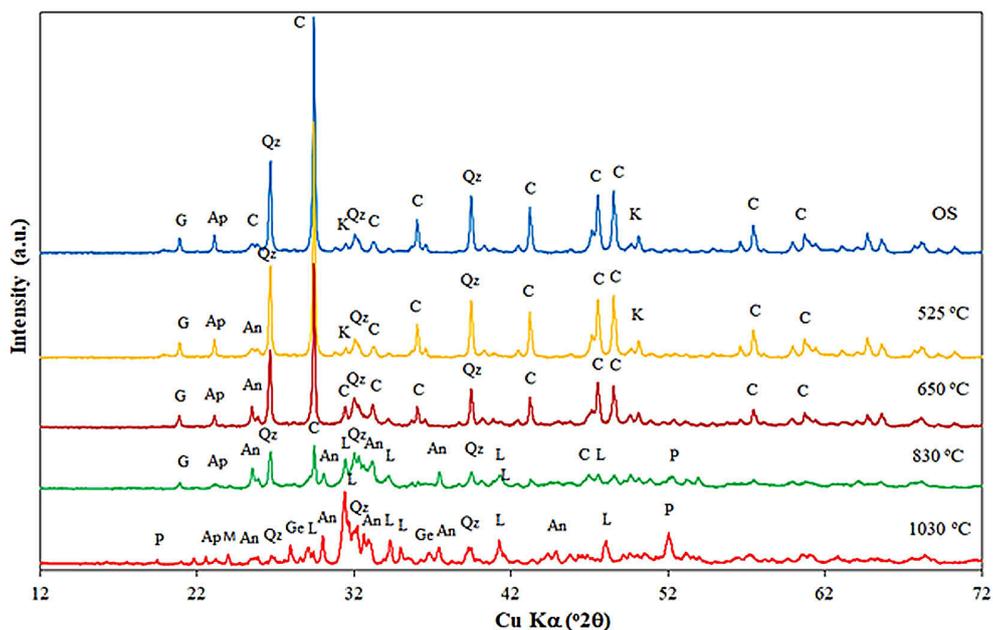**Note:** xxxx – major, xxx – minor, x – trace.

Figure 3. XRD analysis of the El-Lajjun oil shale and ashes obtained at burning oil shale at various temperatures
Note: Q – Quartz (SiO_2), C – Calcite ($CaCO_3$), An – Anhydrite ($CaSO_4$), L – Lime (CaO), P – Portlandite ($Ca(OH)_2$), G – Gehlenite ($Ca_2Al_2SiO_7$), M – Magnetite (Fe_3O_4).

As the combustion temperature increased, the 2θ of different peaks varied vaguely in the peaks of the XRD spectra of the residues of burned samples, while the intensity of the peaks decreased. With increasing burning temperature, the crystal structure of the oil shale minerals was changed, causing a variation in 2θ and the quartz and micas peaks. The calcium carbonate peaks reduced when the temperature increased, from 500 to 750 °C, and basically disappeared at 830 °C. The XRD spectrum reflects that the crystalline structure of the kaolinite in the oil shale was decomposed and disappeared at 650 °C (Gougazeh, 2022). When the combustion temperature gradually increased above 650 °C, the intensity of XRD peaks of quartz was much stronger due to the decomposition and disappearance of kaolinite and metakaolin (Gougazeh and Buhl, 2014). At 1030 °C, the intensity of quartz peaks became clearly stronger with the exception of most minerals, which weakened significantly, and indicated that the temperature had a noticeable effect on the mineral structure as well as inorganic composition consisting of oil shale materials.

FTIR spectroscopy

Figure 4 shows the FTIR absorption peak of the raw oil shale and obtained oil shale ash at various temperatures as well as the considerable variation in the position and the intensity of the main calcite absorption peaks between oil shale

and various OSA materials produced (mainly recarbonated lime). Functional groups in these spectra have been shown to be able to identify the changes in the oil shale structure during calcination. The characteristic peaks of kerogen and inorganic minerals were presented in Table 3. The different conditions of –OH induced various bond lengths and different peak values appeared in the spectra. Two strong bands at 3698 cm^{-1} and 3621 cm^{-1}, individually, belonged to the vibration absorption of exogenous hydroxyl and endogenous hydroxyl. Because the –OH axis of endogenous hydroxyl is nearly parallel with the layer, the vibration frequency of this hydroxyl is low. The peak at 3655 cm^{-1} is the result of the combination of two medium-strength hydroxyl absorption peaks, which were induced by the stretching vibration absorption of exogenous hydroxyl (Ballan et al., 2001; Gougazeh and Buhl, 2010). The peak at 1415 cm^{-1} represents the curved vibration of –OH and the peak at 913 cm^{-1} at the average energy level corresponds to the oscillate absorption of external hydroxyl. With the heating temperature reaches 750 °C, peak of hydroxyl absorption disappeared, indicating that the crystalline water in oil shale has decreased to the disappearance point with an increase in temperature.

In the low-band region, the adsorption peak of minerals was a major one, and the peak of Si–O asymmetric stretching vibration occurs between 1034 cm^{-1} and 1090 cm^{-1}, which reveals that the oil shale materials contain abundant minerals.
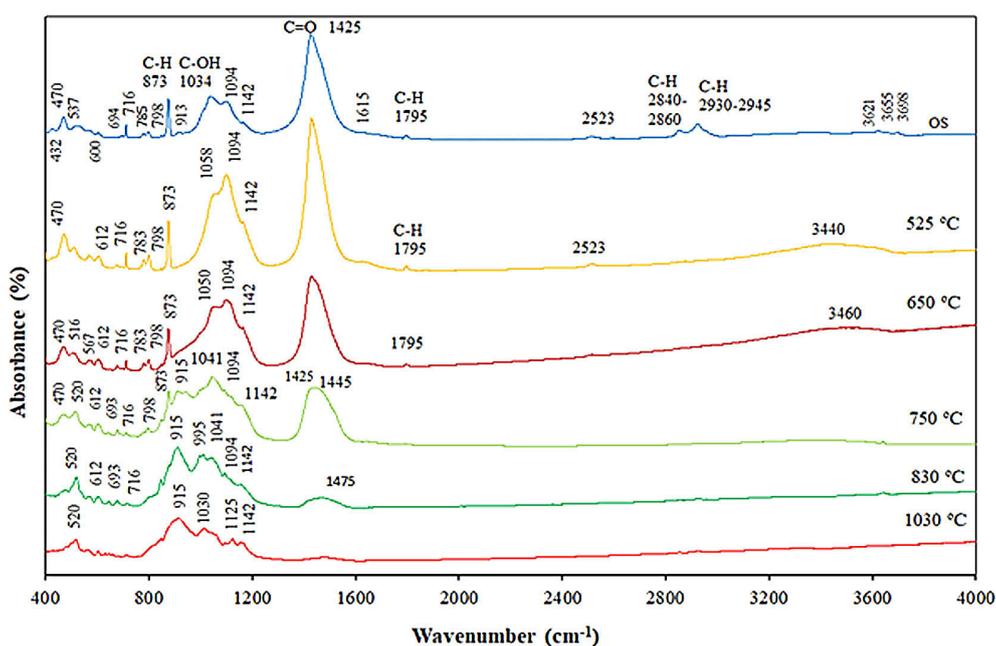

Figure 4. FTIR spectra of raw El-Lajjun oil shale and their oil shale ash treated at various temperatures

The consecutive peaks with very low intensities appear between 900 and 567 cm^{-1} show the C–H and C-C bending vibrations for aromatic structures. Weak shoulders at about 1125 and 600 cm^{-1} point insubstantial sulfate content in the El-Lajjun oil shale. Moderate intensities of adsorption bands range 2860–2930 cm^{-1} belong to the aliphatic stretching C–H vibrations of CH$_3$ and CH$_2$ groups, respectively. From Figure 4 and Table 3 it is clear that the peaks of 2930 and 2860 cm^{-1} are associated to the complete disappearance of organics above 525 °C, indicating that organic matter is not completely cracked at 525 °C. On the other hand, it is also indicated that some reactions occur only when the temperature is higher than 525 °C, which may also be the cause of the irregular oil obtained at 525 °C. As it is shown in Figure 4, the IR spectrums have pointed out a relatively sharp peak at 1425 cm^{-1} with a relatively strong intensities due to the C=O stretching vibrations of carbonyl, especially carboxyl groups, which refer to the fulvic character. Considering the FTIR spectrum, the El-Lajjun oil shale is distinguished by a high amount of organic functional groups, mainly including aliphatic and aromatic compounds.

In addition, the absorption peaks of the C–O functional groups and minerals initially increased at first and then tended to decline. This pointed out that as the temperature rises, there has been a series of complex interactions, including: oxidation, dehydroxylation, dehydrogenation, and condensation, which were temperature dependent. Figure 4 illustrates the contrast in the content of functional groups in the El-Lajjun oil shale as the temperature rises. The C–O content has fluctuated in oil shale from room temperature to 1030°C. In raw oil shale, the C–O content was nearly 200 a.u. and diminished to 100 a.u. (Fig. 4) when the heating temperature increased to 650 °C. However, the C–O content increased considerably between 525 and 650 °C. This can be demonstrated by decomposing and generating groups containing oxygen in oil shale. In the first phase of heating, the content of functional groups containing oxygen decreased, while more new groups were produced when the temperature increased. By contrast, a slight decline of C=C, –OH, and –CH$_2$– can be observed, which suggested that these groups were gradually damaged during the heating process.

Combining Figures 3 and 4, when the heating temperature rose to 525 °C, the low range of

Table 3. Main distinctive peaks in FTIR spectra for the main inorganic minerals

Component	Wavenumber (cm^{-1})
Calcite	2520, 1800, 1430, 872, 742, 716, 697, 694
Quartz	1088, 798, 780, 778
Kerogen (OM)	2924, 2928, 2850, 2852, 1750, 1625, 1460, 1000-1030
Kaolinite	3710, 3650
Silicate	1440, 530, 470

kaolinite band in the high-frequency zone indicated that the kaolinite had begun to lose the hydroxyl in the structure. However, the main ranges of SiO$_2$ at 1094 cm^{-1}, 798 cm^{-1}, 694 cm^{-1}, and 470 cm^{-1} are still present (Table 3). As the temperature constantly increases, the rate of hydroxyl strength for infrared absorption bands caused by stretch vibration and curved vibration.

Thermal analysis

Figure 5 illustrates the analysis of thermal curves (TGA and DTA) of the examined El-Lajjun oil shale. The mass loss of the investigated oil shale was calculated using the thermogravimetric curve, whereas the differential thermal analysis curve (DTA) is based on the change of thermal content in the studied sample, either exothermic or endothermic (transformations with the increasing temperature).

Figure 5 shows a significant total mass loss of about 43 wt.%, including organic matter, kaolinite, and carbonate decomposition. It was noted that the heating experiment consists of three stages. The lower temperature occurs up to 200 °C, produced a maximum of 1 wt.% of the initial mass. This can mainly be due to loss of moisture. The second, relatively high weight loss in the temperature region shows from 200 to 600 °C, which is a significant losing in the mass (~22 wt.%). This was assigned to heat-based decomposition of organic substances, including bitumen and kerogen. The second stage is a region that produces oil through temperature decomposition of organic material in oil shale and crystalline water release in the kaolin minerals (Bai et al., 2015; Gougazeh and Buhl, 2010; Gougazeh, 2022). The third mass loss was observed between 600 and 850 °C, with a total loss of about 20 wt.%. This region is associated with the decomposition of carbonates (high calcite content), a highly endothermic reaction.
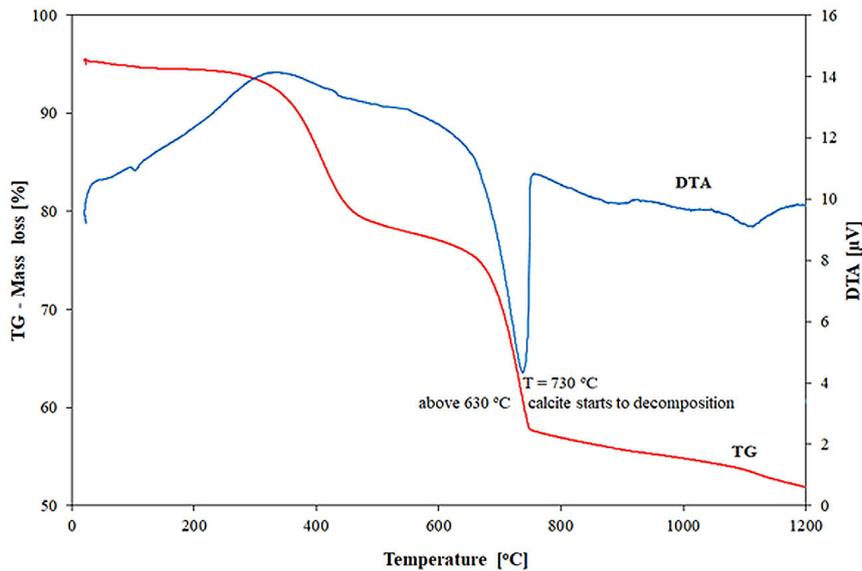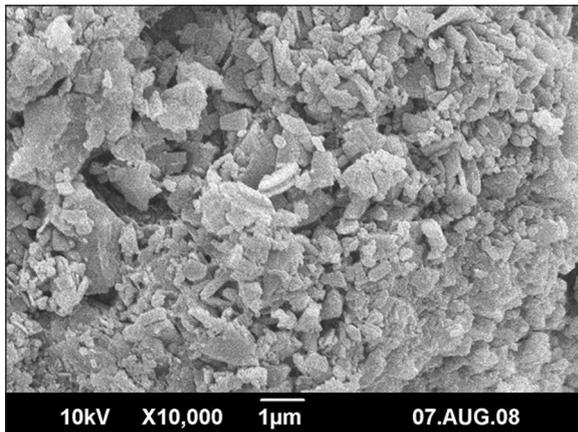
Figure 5. TG and DTA curves of the El-Lajjun oil shale

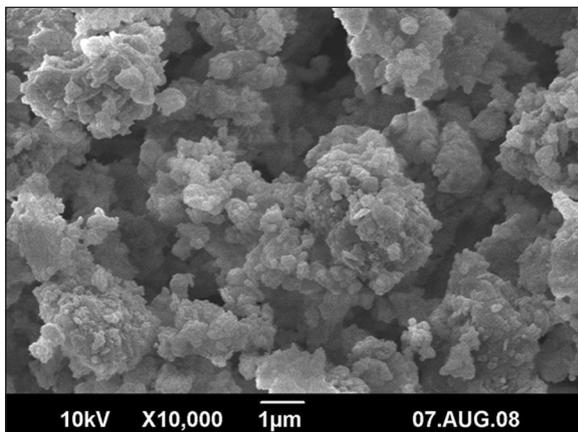**Figure 6.** SEM micrograph, large crystals of calcite ($CaCO_3$)

Figure 7. SEM micrograph of oil shale ash was burned at 830 °C, and most of the calcite crystals are completely converted into lime

Crystal morphology (SEM studies)

Scanning electron microscopy is mainly used to scan and characterize the macropores which contribute less to the specific surface area. Figures 6 and 7 summarize the SEM findings and provide micrograph images of oil shale and oil shale ash, respectively. As shown in Figure 7, the lime particles resulting from the burning process above 830 °C showed the lumpy morphology of the circular or the pleospheres. The findings on SEM/EDX are in accordance with the observations from XRD.

CONCLUSIONS

From the data obtained in this study, it is possible to draw some conclusions of great importance. The FTIR and XRD results are combined in determining the inorganic mineral composition of oil shale and oil shale ash when it comes to the crystallized contents of inorganic mineral of oil shale, especially in determining carbonate minerals. The FTIR results indicated that all kerogen may be oxidized by hydrogen peroxide and that aliphatic compounds are the most hydrocarbons found in the oil shale. The TGA weight loss was calculated on mineral decomposition content between 20 and 1000 °C. The composition of inorganic matter of the investigated oil shale consisted mainly of calcite and quartz with traces of gypsum, kaolinite,

apatite and magnetite, while the shale ash obtained above 830 °C consisted mainly of quartz, lime, anhydrite and amorphous phases with minor amounts of portlandite and gehlenite.

Acknowledgements

Funding

REFERENCES

1. Abed A.M., Arouri K., Amiereh B.S., Al-Hawari Z. 2009. Characterization and genesis of some Jordanian oil shales. Dirasat, Pure Sciences, 36(1), 7–17.

2. Ballan E., Marco Saitta A., Mauri F., Galas G. 2001. First-principles modeling of the infrared spectrum of kaolinite. American Mineralogist, 86, 1321–1330.

3. Bai F.T., Wei G., Lu X.S., Liu Y.M., Guo M.Y., Li Q., Sun Y.H. 2015. Kinetic study on the pyrolysis behavior of Huadian oil shale via non-isothermal thermogravimetric data. Fuel, 146, 111–118.

4. Bender F. 1974. Geology of Jordan. Contribution to the regional geology of the world. Gebrueder Borntraeger, Berlin, Germany, 196.

5. Bseieso M.P. 2003. Jordan's experience in oil shale studies employing different technologies. Oil Shale, 20(3), 360–370.

6. Gougazeh M., Buhl J. Ch. 2010. Geochemical and mineralogical characterization of the Jabal Al-Harad kaolin deposit, southern Jordan, for its possible utilization. Clay Minerals, 45, 281–294.

7. Gougazeh, M., Buhl J.-Ch. 2014. Synthesis and characterization of zeolite A by the hydrothermal transformation of natural Jordanian kaolin. Journal of the Association of Arab Universities for Basic and Applied Sciences, 15, 35–42.

8. Gougazeh M. 2020. Beneficiation Study of Low-Grade Jordanian Kaolin to Increase the Brightness Index. Jordan Journal of Civil Engineering, 14(3), 319–3309.

9. Gougazeh M. 2022. Beneficiation and upgrading of Jordanian oil shale. Physicochemical Problems of Mineral Processing, 58(3), 147092.

10. Hamarneh Y. 1988. Oil Shale Deposits in Central Jordan: Ministry of Energy and Mineral Resources. Amman, Jordan.

11. Hruljova J., Savest N., Oja V., Suuberg E.H. 2013. Kukersite oil shale kerogen solvents welling in binary mixtures. Fuel, 105, 77–82.

12. Khraisha Y.H., Irqsousi N.A., Shabib I.M. 2003. Spectroscopic and chromatographic analysis of oil from an oil shale flash pyrolysis unit. Energy Conversion and Management, 44, 125–135.

13. Larsen J.W., Parikh H.M., Michels R., Raoult N., Pradier B. 2000. Kerogen macromolecular structure. Preprints Symposium American Chemical Society, Division of Fuel Chemistry, Dallas, TX (USA), 45, 211–215.

14. Saikia B.K., Ward C.R., Oliveira M.L.S., Hower J.C., Leao F.D., Johnston M.N., O'Bryan A., Sharma A., Baruah B.P. Silva L.F.O. 2015a. Geochemistry and nano-mineralogy of feed coals, mine overburden, and coal-derived fly ashes from Assam (Northeast India): A multi-faceted analytical approach. International Journal of Coal Geology, 137, 19–37.

15. Shaohui G. 2000. Solvent extraction of Jordanian oil shale kerogen. Oil Shale, 17(3), 266–670.